

Improved Rodent Model of Myocardial Ischemia and Reperfusion Injury

Hua-Qin Tong^{*,1,2,3}, Man-Lu Fan^{*,3}, Tong Sun³, Hao-Wen Zhang⁴, Jie Han⁵, Meng-Xi Wang³, Jian-Dong Chen⁵, Wei-Xin Sun⁶, Xiao-Hu Chen^{1,2}, Mian-Hua Wu⁷

¹ Department of Cardiology, Affiliated Hospital of Nanjing University of Chinese Medicine ² Department of Cardiology, Jiangsu Province Hospital of Chinese Medicine ³ First College of Clinical Medicine, Biological Technology Center for Innovation in Chinese Medicine, Nanjing University of Chinese Medicine ⁴ School of Health Preservation and Rehabilitation, Key Laboratory of Acupuncture and Medicine Research of Ministry of Education ⁵ Department of Cardiology, Jiangsu Provincial Hospital of Chinese Medicine ⁶ Department of Cardiology, Yancheng TCM Hospital Affiliated to Nanjing University of Chinese Medicine ⁷ Jiangsu Collaborative Innovation Center of Traditional Chinese Medicine (TCM) Prevention and Treatment of Tumor, Nanjing University of Chinese Medicine

* These authors contributed equally

Corresponding Authors

Xiao-Hu Chen

chenxhdoctor@sina.com

Mian-Hua Wu

wmh@njucm.edu.cn

Citation

Tong, H.Q., Fan, M.L., Sun, T., Zhang, H.W., Han, J., Wang, M.X., Chen, J.D., Sun, W.X., Chen, X.H., Wu, M.H. Improved Rodent Model of Myocardial Ischemia and Reperfusion Injury. *J. Vis. Exp.* (181), e63510, doi:10.3791/63510 (2022).

Date Published

March 7, 2022

DOI

10.3791/63510

URL

jove.com/video/63510

Introduction

Ischemic heart disease is the leading cause of mortality worldwide. Cardiovascular mortality has a crucial role in public health and epidemiology globally¹. Myocardial

ischemia and reperfusion injury play essential functions in ischemic heart disease, which refers to a complex pathophysiological process that includes depletion of

Abstract

Myocardial ischemia and reperfusion injury (MIRI), induced by coronary heart disease (CHD), causes damage to the cardiomyocytes. Furthermore, evidence suggests that thrombolytic therapy or primary percutaneous coronary intervention (PPCI) does not prevent reperfusion injury. There is still no ideal animal model for MIRI. This study aims to improve the MIRI model in rats to make surgery easier and more feasible. A unique method for establishing MIRI is developed by using a soft tube during a key step of the ischemic period. To explore this method, thirty rats were randomly divided into three groups: sham group (n = 10); experimental model group (n = 10); and existing model group (n = 10). Findings of triphenyltetrazolium chloride staining, electrocardiography, and percent survival are compared to determine the accuracies and survival rates of the operations. Based on the study results, it has been concluded that the improved surgery method is associated with a higher survival rate, elevated ST-T segment, and larger infarct size, which is expected to mimic the pathology of MIRI better.

adenosine triphosphate², excessive generation of reactive oxygen species³, inflammatory reactions⁴, and mitochondrial dysfunction owing to calcium overload⁵, which triggers acute myocardial infarction *via* metabolic dysfunction and structural damage⁶.

However, the detailed mechanisms underlying myocardial ischemia and reperfusion injury (MIRI) remain unknown. The present work aims to develop a unique animal model that adequately simulates the clinical presentation and treatment of MIRI. Otherwise, in the process of MIRI model research, large animals⁷ (such as pigs) require interventional surgery, which is expensive. Small animals (such as rabbits⁸, mice^{9,10,11,12}, and rats¹³) require delicate surgery under microscopy¹⁰, remote-controlled saccules^{8,11}, or squeezing the heart out of the cavity⁹, which requires a high level of technology and may cause several postoperative complications that disturb the accuracy of findings. An ideal MIRI model with a higher survival rate and lower cost will play a crucial role in pathological research.

This study aimed to combat these issues by establishing a more accessible and feasible model of MIRI in rats to facilitate the research on the pathology of MIRI, which could lead to the discovery of clinical therapies for MIRI.

Protocol

The study was approved by the Animal Care and Use Committee of the Nanjing University of Chinese Medicine (permission no. 202004A002). The study strictly followed the National Institutes of Health (NIH) guidelines on the Use of Laboratory Animals (NIH publication No. 85-23, revised 2011). Thirty male Sprague-Dawley rats (weight, 300 ± 50 g; age, 12 ± 14 weeks) were used in this work.

1. Animal preparation

1. Deprive the rats of food and water for 12 h before surgery. Preoperative fasting aims to prevent pulmonary aspiration¹⁴.
2. Sterilize all instruments before surgery using a high-pressure steam sterilizer.
3. Anesthetize the rats by administering pentobarbital sodium (1.5%, 75 mg/kg) *via* intraperitoneal injection (see **Table of Materials**).
4. Assess the effectiveness of anesthesia by performing the pinch-toe test.
NOTE: The rat is considered sufficiently anesthetized if no reflexes are observed when its hind paw is held by the tweezers.
5. Straighten the middle section of two paper clips to form an "S" shape. Pull down the wide section of each "S" to form a small retractor.
6. Cut a 2 mm diameter polyvinyl chloride (PVC) tube into 7 mm-length pieces. Insert a 10 cm long 4-0 suture into the PVC tube, and tie its ends.
7. Ligate the left anterior descending (LAD) coronary artery and the PVC tube together using a 6-0 suture. Cut a groove in the middle of the PVC tube using ophthalmic scissors, and use the groove to thread the 6-0 suture through the tube to prevent it from falling off.

NOTE: The PVC tube and "S" shape retractors are shown in **Supplementary Figure 1**.

2. Surgery procedure

1. Perform surgery to generate the improved MIRI rat model following the steps below.

NOTE: The animal model group generated by the improved MIRI method is referred to as the experimental model group throughout the article.

1. After anesthesia (step 1.2), fix the limbs of the rat with tape by placing the rat on the surgical board in the supine position. Shave the neck and left anterior chest area with depilatory cream, and clean the skin with 75% alcohol and iodophor scrub.

2. Cut the skin of the neck lengthwise along the median cervical line using ophthalmic scissors.

3. Separate the neck muscles using ophthalmic tweezers, and place a retractor (step 1.4) on each side to retract them further.

NOTE: It is necessary to expose the trachea adequately, as it is critical for preventing bleeding from the thyroid gland during this step.

4. After exposing the trachea, identify the space between the fourth and fifth tracheal rings. This space is the puncture point.

5. Mark this point using the blunt edge of a needle tip. Make a 3 mm incision parallel to the cricoid cartilage at this point.

6. Insert a suction trocar (see **Table of Materials**) into the trachea *via* the incision (step 2.1.5), and mechanically ventilate the rat to maintain normal respiration at a rate of 80 breaths/min and a tidal volume of 8 mL/kg.

7. Next, make a 4-5 cm incision from the xiphoid to the middle of the second left intercostal space while holding the scalpel at a 45° angle. Gently and slowly, separate the pectoralis major and serratus anterior muscles using ophthalmic tweezers to access the intercostal space.

8. Make a 1.5 cm incision transversely between the left third and fourth ribs using ophthalmic scissors.

9. If required, cut out the fourth rib to expose the heart covered by the left lung. This gives better visibility.

10. To prevent injuries, place cotton balls soaked in the physiological saline solution above the lungs in the thoracic cavity. Dissect the pericardium using ophthalmic tweezers, lift the left atrial appendage by tweezers, and identify the coronary ostium present at the root of the aortic artery.

11. In the section between the left lung and auricle, ligate the LAD and the pre-prepared short tube (step 1.6) together using a 6-0 surgical suture, and tie it using a slipknot. Place the slipknot in the groove of the PVC tube, and tighten the ligated tube and LAD using a second slipknot for 45 min¹⁵ (**Figure 1A,B**).

12. Record the color change in the anterior part of the left ventricle and ST-segment elevation on electrocardiogram (ECG) during the ischemia period.

NOTE: The anterior part of the left ventricle turns pale during the ischemia period.

13. Clamp the chest muscles and skin using an artery clip, and cover the wound with moist saline gauze.

14. Loosen the slipknot, and remove the pre-prepared short tube after 45 min¹⁵ (**Figure 1C**).

15. Keep the rats anesthetized during reperfusion for 2 h.

2. Perform surgery to generate the rat model following the previously published procedure¹⁶.

NOTE: This animal model group is referred to as the existing model group throughout the article.

1. Before ligation of the LAD coronary artery, perform the same steps as the experimental model group.
2. During the ischemic period, ligate each rat's proximal LAD coronary artery with a slipknot only using a 6-0 surgical suture at the same position as the experimental model group and tie a slipknot for 45 min.
3. After the ligation, loosen the slipknot with tweezers, suture the incisions of the rat with a suture needle and tweezers, and keep the animal in deep anesthesia of 1.5% pentobarbital sodium throughout the period of reperfusion^{17,18,19} for 2 h before harvesting the rat's hearts.

3. Assessment of triphenyltetrazolium chloride staining

1. At the end of reperfusion, the rats are euthenized while still deeply anesthetized. Sacrifice the rats and harvest their hearts^{16,20} immediately. Wash the hearts in PBS solution, and store them at $-20\text{ }^{\circ}\text{C}$ for ~ 20 min to harden the tissues.
2. Subsequently, cut the hearts into 2 mm slices with a microtome blade, incubate them with 2% triphenyltetrazolium chloride (TTC) (see **Table of Materials**) at $37\text{ }^{\circ}\text{C}$ for ~ 30 min, and fix them in 10% neutral formalin.
3. Photograph the heart slices, and calculate the infarct areas using an image processing program of ImageJ software (see **Table of Materials**).

NOTE: Due to the staining, the infarct sites appear pale white, whereas normal tissues appear dark red.

4. Histological staining

1. Harvest the hearts under deep anesthesia of 1.5% pentobarbital sodium at the end of the reperfusion period.
2. Fix the hearts in 10% formalin at $4\text{ }^{\circ}\text{C}$ for 48 h.
3. Subsequently, section the hearts with a microtome into at least 6 slices ($5\text{ }\mu\text{m}$ thick) and ensure at least three slices for hematoxylin and eosin (H&E) and Masson staining^{20,21}.
4. Observe the slides under a light microscope, and photograph them.

5. ECG assessment

1. Randomly divide animals into experimental or existing MIRI model groups or sham groups to assess the ECG changes.
2. Anesthetize all rats during the surgical ligations and assess standard limb lead II tracing^{20,21} to identify ECG changes and confirm myocardial ischemia.
3. Store all images in a digital library.

6. Statistical analysis

1. Perform statistical analyses using scientific graphing and statistics software (see **Table of Materials**).
2. Express all data as mean \pm standard error of the mean. After normality and lognormality tests of each group, perform a one-way analysis of variance and t-tests²² to determine significant differences among the groups. Consider p -value < 0.05 as statistically significant.

Representative Results

TTC staining

Heart sections from rats that underwent either the existing or improved MIRI procedure or sham surgery were stained with TTC, and the images were stored digitally and analyzed using ImageJ. Rats that underwent either the already existing or improved MIRI procedures had myocardial infarctions, while rats from the sham group did not (**Figure 2B**). Compared to rats in the sham group, rats in the existing ($p < 0.0001$) and experimental ($p < 0.0001$) MIRI model groups had a significant difference in myocardial infarct size, and the experimental model group had a larger myocardial infarct size than the existing model group ($p = 0.0176$) (**Figure 3B**).

Histological staining

Analysis of specimens stained using H&E and Masson stains^{22,23} showed that compared to the sham group, the cardiomyocytes of both the experimental and the existing model groups had experienced critical damage and nucleolysis and were infiltrated by numerous neutrophils (**Figure 3**).

ECG test

The ECG ST-T segments of rats in the existing and experimental MIRI model groups were elevated compared with those of rats in the sham group (**Figure 4A**), and the differences between the experimental model and sham groups ($p < 0.0001$) or the existing model and sham groups ($p < 0.0001$) were significant (**Figure 4B**). Furthermore, the ST-T segment was more elevated in the experimental model group than in the existing model group ($p = 0.0274$) (**Figure 4C**).

Percent survival

The survival rate was significantly different between the two MIRI model groups (**Figure 4D**). Four of the ten rats died in the existing model group. The mortality rate was 40% during the reperfusion period. In contrast, none of the rats in the experimental model group died during surgery, demonstrating that the current improved model had a higher survival rate ($p = 0.0291$).

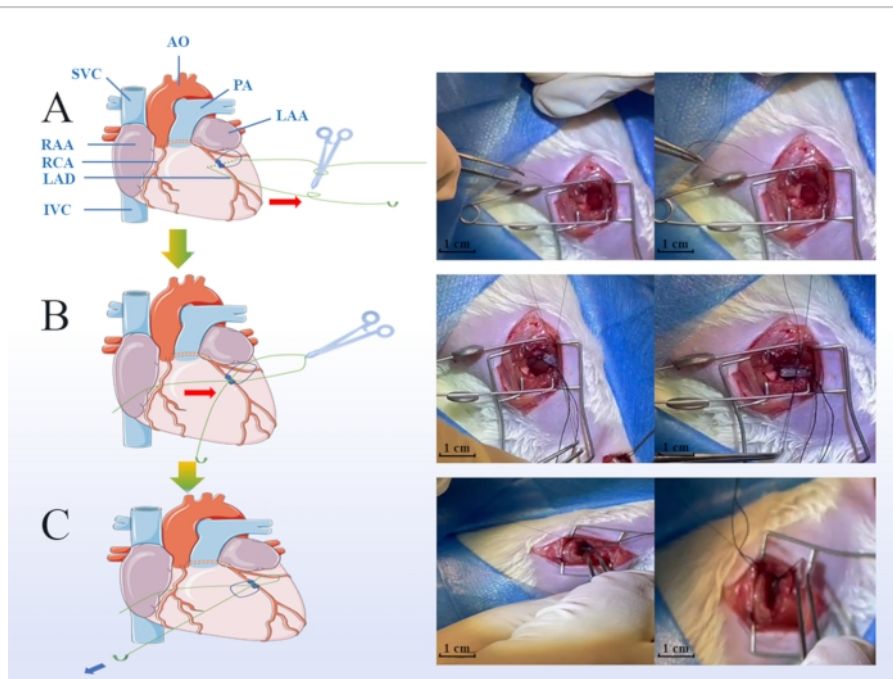


Figure 1: Key steps of the myocardial ischemic and reperfusion injury (MIRI) model surgery. Green points indicate the protocol of ligature during the ischemic period, including placing the soft tube on the coronary arteries (A), hooking the suture line into the groove of the pre-prepared soft tube (B), loosening the slipknot, and removing the soft tube when the reperfusion period was started (scale bar = 1 cm) (C). LAA: Left Atrial Appendage, RAA: Right Atrial Appendage, LAD: Left Anterior Descending, RCA: Right Coronary Artery, IVC: Inferior Vena Cava, SVC: Superior Vena Cava, AO: Aorta Artery, PA: Pulmonary Artery. [Please click here to view a larger version of this figure.](#)

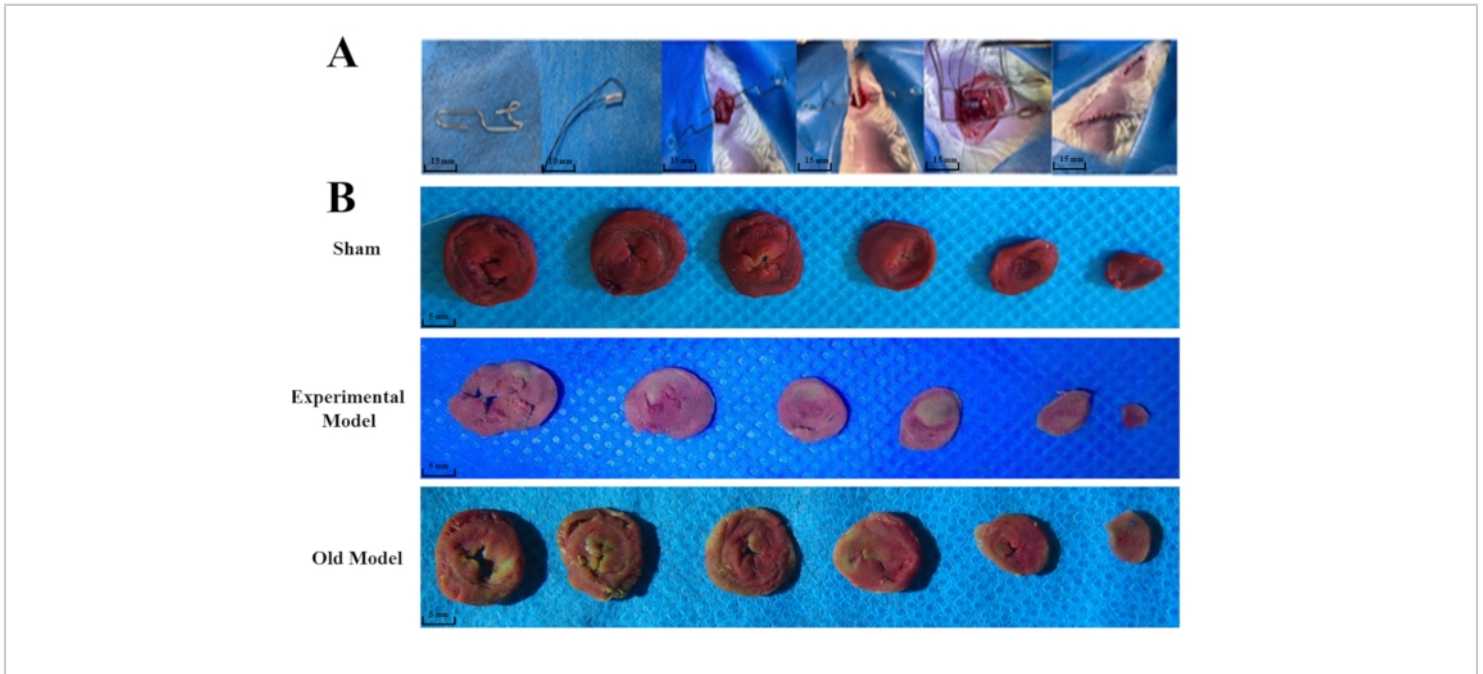


Figure 2: The whole surgery procedure and differences in triphenyltetrazolium chloride (TTC) staining between different groups. The pre-prepared small retractor (scale bar = 15 mm), soft tube (scale bar = 10 mm), and the whole surgery (scale bar = 15 mm) are shown (A). Thirty rats were randomly divided into the experimental (n = 10), sham group (n = 10), and existing model (n = 10) groups. TTC staining indicated that both the experimental and existing models' groups had significant changes compared to the sham group (B). The anterior wall of the myocardium in the experimental and the lateral wall in the existing model groups turned pale white, confirming the ischemic area's location (scale bar = 5 mm). The "existing model" is depicted as the "old model" in the figure. [Please click here to view a larger version of this figure.](#)

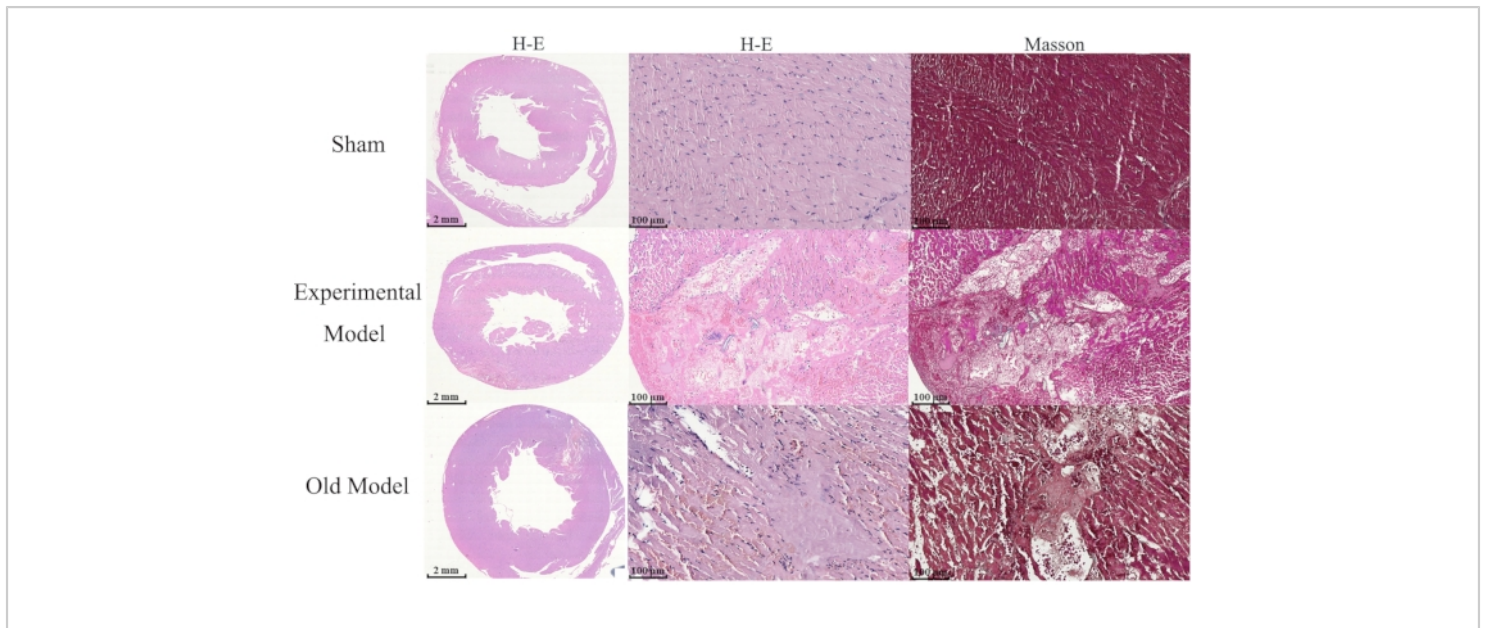


Figure 3: Differences in H&E and Masson staining between groups. Thirty male Sprague Dawley rats were randomly divided into the experimental (n = 10), sham group (n = 10), and existing model (n = 10) groups, and the comparison of cell morphological changes between groups is shown (scale bar = 2 mm). Hematoxylin and Eosin (H&E), and Masson staining show that myocardial cells of the experimental model and existing model groups have critical damage, nucleolysis, and are infiltrated by numerous neutrophils compared to those of the sham group (scale bar = 100 μm). The "existing model" is depicted as the "old model" in the figure. [Please click here to view a larger version of this figure.](#)

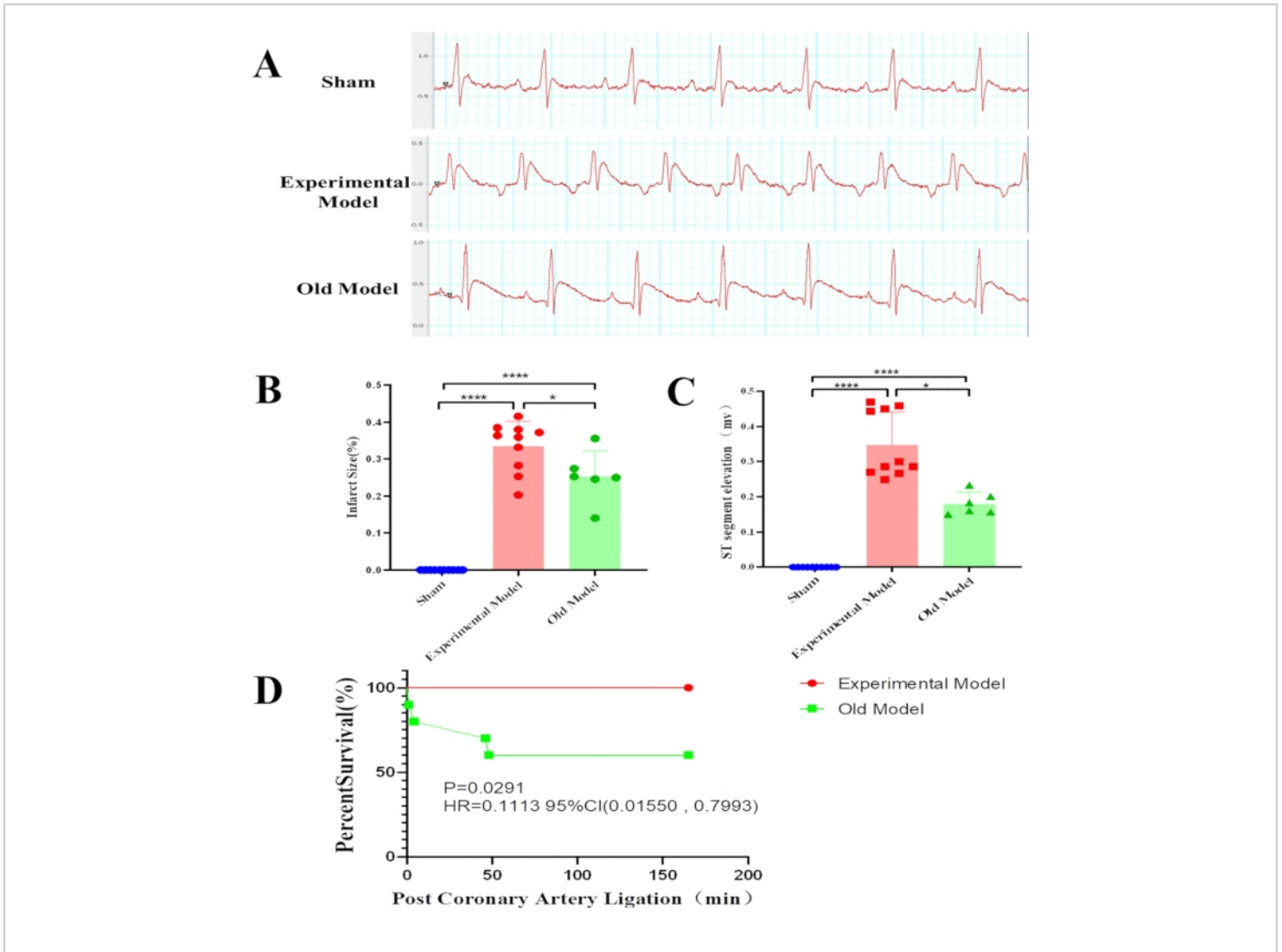


Figure 4: Differences in statistical results between groups. Thirty male Sprague Dawley rats were randomly divided into the experimental (n = 10), sham group (n = 10), and existing model (n = 10) groups. Electrocardiogram findings show that compared to the already existing model group, the experimental model group has a larger myocardial infarct size ($****p < 0.0001$, $*p = 0.0176$) (A), a higher ST-segment elevation ($****p < 0.0001$, $*p = 0.0274$) (B), and a higher survival percentage ($p = 0.0291$) (C). Especially, rats of the existing model group were more likely to die at the beginning of the ischemia period and the beginning of the reperfusion period (D). The "existing model" is depicted as the "old model" in the figure. [Please click here to view a larger version of this figure.](#)

Supplementary Figure 1: The details of the pre-prepared retractor and PVC tube. The pre-prepared retractor (A) and PVC tube (B) are shown. [Please click here to download this File.](#)

Discussion

The main difference between the already existing and improved methods was the use of PVC tubes in the ligation process. In the existing surgery method, the myocardial

tissue was ligated using the 6-0 silk suture only, which induced damage to the myocardium during ligation resulting in intraoperative death. Moreover, the pulsation of the heart would loosen the slipknot. In contrast, in the improved method with the PVC tube, the slipknot placed in the groove of the tube could be tightened, and the area of the myocardium affected by ligation increased. These benefits were observed during the experimental procedure and confirmed by the TTC staining and percent survival findings.

The critical step of the improved surgery method was placing the soft tube on the proximal LAD coronary artery, accompanied by nerves, lymphatic vessels, and myocardial tissue during ligation in the ischemic period. This pre-prepared soft tube can act as a cushion that protects the peripheral tissues (nerves, myocardia, and lymphatic vessels) and decreases mortality during coronary artery ligation. The surgery performed by the already existing method was similar to the surgery for myocardial infarction. The percent survival findings indicated that rats in the existing model group mainly died during the ischemic period (two rats died at 2 min post-ligation, and two rats died at 45 min post-ligation). Otherwise, the underlying causes of death are still unclear, and there are a series of hypotheses, including additional damage to the nervous structures²³, lymphatic vessels, and myocardia.

Regarding nervous damage, previous studies have indicated that during the ischemic period in the animal model, besides the direct local effects of ischemia on the nervous structures, there is also probably a significant decrease in neuropeptide Y (NPY) levels that contribute to disturbances in axoplasmic transport in the sympathetic innervation²⁴. This finding agrees with results reported by Han et al.²⁵, who revealed that a gradual disappearance of NPY occurred within the infarcted myocardium after ligation of the LAD coronary

artery in rats. However, the role of NPY in this context remains unclear. Its deletion attenuates cardiac dysfunction and apoptosis during acute myocardial infarction²⁶, and is associated with arrhythmia²⁷, high blood pressure, and coronary microvascular function²⁸.

Furthermore, adverse obstruction of cardiac lymph flow occurred during the ischemic period, leading to severe cardiac edema, left dysfunction, and hemorrhages²⁹, which might be another cause of death in rats. During this pathological process, the ligation of the LAD coronary artery might be attributed to the obstruction of coronary arteries or cardiac lymphatic transport within the infarct area, which can cause additional complications, such as adverse remodeling of the epicardial collector lymphatics, reduced lymphatic flow, and persistent edema³⁰.

Therefore, circulation in lymphatic vessels plays a functional role in cardiac homeostasis³¹ and wound healing³², and the percent survival findings in this study suggest that the improved MIRI surgical procedure might avoid lymphatic damage and promote lymphatic reperfusion by placing the soft tube on the LAD coronary artery during ligation. In comparison, the existing surgery method is more likely to tear the heart muscle and cause a massive hemorrhage during ligation of the LAD coronary artery, without the cushioning effect of the soft tube. Additionally, the pre-prepared soft tube diameter was much larger than the 6-0 silk suture, and the tube may have contracted and induced a larger infarct size when the slipknot was tied to the tube during the ischemic period.

This study had a few limitations. The infarct size of the heart was analyzed in the preliminary experiment. The substitution formula ($N = 7.75$) was calculated using a previously reported equation³³. Considering the possible death of rats during

the operation, N was raised by 25%; hence, n = 10 (ten rats for each group) was decided. Otherwise, the already existing method to generate the MIRI model had a high mortality rate. Therefore, few cases (low sample size) in the experimental model group influenced the statistical findings. Several assessments, including echocardiography³⁰, Evans blue staining³⁴, and the myocardial enzyme measurement³⁵, were essential for cardiac function evaluation and analysis. Owing to the low sample size of this work, these assessments were not performed and will be described in a future study of pharmacodynamic research in MIRI. However, considering that the existing surgical procedure to generate the MIRI model is associated with extensive myocardial damage, it is worthwhile to report this present method to improve the modeling of MIRI in rats and bring light to this preclinical model that correctly simulates ischemic heart disease.

In conclusion, the improved surgery method to generate the MIRI model had a higher survival rate, an elevated ST-T segment, and a larger infarct size than the existing MIRI model generation method, suggesting that the improved model better simulates MIRI pathology.

Disclosures

The authors have nothing to disclose.

Acknowledgments

This work was supported by the Administration of Traditional Chinese Medicine [SLJ0204], the Jiangsu Provincial Hospital of Chinese Medicine (Y21017), the National Natural Science Foundation of China [81973763, 81973824, 82004239].

References

1. Mozaffarian, D., et al. Heart disease and stroke statistics-2016 update: a report from the American heart association. *Circulation*. **133** (4), e38-360 (2016).
2. Allen, D. G., Orchard, C. H. Myocardial contractile function during ischemia and hypoxia. *Circulation Research*. **60** (2), 153-168 (1987).
3. Ashraf, M. I. et al. A p38MAPK/MK2 signaling pathway leading to redox stress, cell death and ischemia/reperfusion injury. *Cell Communication and Signaling*. **12**, 6 (2014).
4. Hernandez-Resendiz, S. et al. The role of redox dysregulation in the inflammatory response to acute myocardial ischaemia-reperfusion injury - adding fuel to the fire. *Current Medicinal Chemistry*. **25** (11), 1275-1293 (2018).
5. Heidrich, F. et al. The role of phospho-adenosine monophosphate-activated protein kinase and vascular endothelial growth factor in a model of chronic heart failure. *Artificial Organs*. **34** (11), 969-979 (2010).
6. Shen, Y., Liu, X., Shi, J., Wu, X. Involvement of Nrf2 in myocardial ischemia and reperfusion injury. *International Journal of Biological Macromolecules*. **125**, 496-502 (2019).
7. Hinkel, R. et al. AntimiR-21 prevents myocardial dysfunction in a pig model of ischemia/reperfusion injury. *Journal of the American College of Cardiology*. **75** (15), 1788-1800 (2020).
8. Torrado, J. et al. Sacubitril/Valsartan averts adverse post-infarction ventricular remodeling and preserves systolic function in rabbits. *Journal of the American College of Cardiology*. **72** (19), 2342-2356 (2018).

9. Guan, L. et al. MCU Up-regulation contributes to myocardial ischemia-reperfusion Injury through calpain/OPA-1-mediated mitochondrial fusion/mitophagy Inhibition. *Journal of Cellular and Molecular Medicine*. **23** (11), 7830-7843 (2019).
10. Fan, Q. et al. Dectin-1 contributes to myocardial ischemia/reperfusion injury by regulating macrophage polarization and neutrophil infiltration. *Circulation*. **139** (5), 663-678 (2019).
11. Huang, C. et al. Effect of myocardial ischemic preconditioning on ischemia-reperfusion stimulation-induced activation in rat thoracic spinal cord with functional MRI. *International Journal of Cardiology*. **285**, 59-64 (2019).
12. Li, D. et al. Cardioprotection of CAPE-oNO₂ against myocardial ischemia/reperfusion induced ROS generation via regulating the SIRT1/eNOS/NF-κB pathway in vivo and in vitro. *Redox Biology*. **15**, 62-73 (2018).
13. Cui, Y., Wang, Y., Liu, G. Protective effect of Barbaloin in a rat model of myocardial ischemia reperfusion injury through the regulation of the CNPY2PERK pathway. *International Journal of Molecular Medicine*. **43** (5), 2015-2023 (2019).
14. Lin, M. W. et al. Prolonged preoperative fasting induces postoperative insulin resistance by ER-stress mediated Glut4 down-regulation in skeletal muscles. *Int J Med Sci*. **11;18**(5):1189-1197 (2021).
15. Wu, J. et al. Sevoflurane alleviates myocardial ischemia reperfusion injury by inhibiting P2X7-NLRP3 mediated pyroptosis. *Frontiers in Molecular Biosciences*. **26** (8), 768594 (2021).
16. Wu, Y., Yin, X., Wijaya, C., Huang, M. H., McConnell, B. K. Acute myocardial infarction in rats. *Journal of Visualized Experiments*. **48**, e2464 (2011).
17. Zhang, C. X. et al. Mitochondria-targeted cyclosporin: A delivery system to treat myocardial ischemia reperfusion injury of rats. *Journal of Nanobiotechnology*. **17** (1), 18 (2019).
18. Liu, X. M. et al. Long non-coding RNA MALAT1 modulates myocardial ischemia-reperfusion injury through the PI3K/Akt/eNOS pathway by sponging miRNA-133a-3p to target IGF1R expression. *European Journal of Pharmacology*. **916**, 174719 (2022).
19. Li, L. et al. Ginsenoside Rg3-loaded, reactive oxygen species-responsive polymeric nanoparticles for alleviating myocardial ischemia-reperfusion injury. *Journal of Controlled Release*. **317**, 259-272 (2020).
20. Mickelson, J. K. et al. Streptokinase improves reperfusion blood flow after coronary artery occlusion. *International Journal of Cardiology*. **23** (3), 373-84 (1989).
21. Verscheure, Y., Pouget, G., De Courtois, F., Le Grand, B., John, G. W. Attenuation by R 56865, a novel cytoprotective drug, of regional myocardial ischemia- and reperfusion-induced electrocardiographic disturbances in anesthetized rabbits. *Journal of Cardiovascular Pharmacology*. **25** (1), 126-33 (1995).
22. Fan, M. L. et al. Animal model of coronary microembolization under transthoracic echocardiographic guidance in rats. *Biochemical and Biophysical Research Communications*. **568** (3), 174-179 (2021).

23. Lim, M. et al. Intravenous injection of allogeneic umbilical cord-derived multipotent mesenchymal stromal cells reduces the infarct area and ameliorates cardiac function in a porcine model of acute myocardial infarction. *Stem Cell Research & Therapy*. **9** (1), 129 (2018).
24. Trautner, H. et al. Heart innervation after ligation of the left anterior descending coronary artery (LAD). *Histochemistry*. **92** (2), 103-108 (1989).
25. Han, C., Wang, X. A., Fiscus, R. R., Gu, J., McDonald, J. K. Changes in cardiac neuropeptide Y after experimental myocardial infarction in rat. *Neuroscience Letters*. **104** (1-2), 141-146 (1989).
26. Huang, W. et al. Deletion of neuropeptide Y attenuates cardiac dysfunction and apoptosis during acute myocardial infarction. *Frontiers in Pharmacology*. **10**, 1268 (2019).
27. Kalla, M. et al. The cardiac sympathetic co-transmitter neuropeptide Y is pro-arrhythmic following ST-elevation myocardial infarction despite beta-blockade. *European Heart Journal*. **41** (23), 2168-2179 (2020).
28. Cuculi, F. et al. Relationship of plasma neuropeptide Y with angiographic, electrocardiographic and coronary physiology indices of reperfusion during ST elevation myocardial infarction. *Heart (British Cardiac Society)*. **99** (16), 1198-1203 (2013).
29. Vuorio, T., Tirronen, A., Ylä-Herttuala, S. Cardiac Lymphatics - a new avenue for therapeutics. *Trends in Endocrinology and Metabolism: TEM*. **28** (4), 285-296 (2017).
30. Henri, O. et al. Selective stimulation of cardiac lymphangiogenesis reduces myocardial edema and fibrosis leading to improved cardiac function following myocardial infarction. *Circulation*. **133** (15), 1484-1497 (2016).
31. Oliver, G., Kipnis, J., Randolph, G. J., Harvey, N. L. The lymphatic vasculature in the 21st century: novel functional roles in homeostasis and disease. *Cell*. **182** (2), 270-296 (2020).
32. Klotz, L. et al. Cardiac lymphatics are heterogeneous in origin and respond to injury. *Nature*. **522** (7554), 62-67 (2015).
33. Percie du Sert, N. et al. Reporting animal research: Explanation and elaboration for the ARRIVE guidelines 2.0. *PLoS Biology*. **18** (7), e3000411 (2020).
34. Miller, D. L., Li, P., Dou, C., Armstrong, W. F., Gordon, D. Evans blue staining of cardiomyocytes induced by myocardial contrast echocardiography in rats: evidence for necrosis instead of apoptosis. *Ultrasound in Medicine & Biology*. **33** (12), 1988-1996 (2007).
35. Deng, C. et al. α -Lipoic acid reduces infarct size and preserves cardiac function in rat myocardial ischemia/reperfusion injury through activation of PI3K/Akt/Nrf2 pathway. *PLoS ONE*. **8** (3) e58371 (2013).